Pergamon

Int. J. Solids Structures Vol. 34, No. 4, pp. 493–507, 1997

0020–7683/97 $17.00 + .00

PII: S0020–7683(96)00027–3

TRANSVERSELY ISOTROPIC MODULI OF TWO PARTIALLY DEBONDED COMPOSITES

Y. H. ZHAO† and G. J. WENG
Department of Mechanical and Aerospace Engineering, Rutgers University, New Brunswick, New Jersey 08903, U.S.A.

(*Received* 27 *February* 1995; *in revised form* 30 *January* 1996)

Abstract—The effective transversely isotropic moduli of two hybrid composites containing both partially debonded and perfectly bonded spheroidal inclusions are derived. In this derivation a fictitious, transversely isotropic inclusion is introduced to replace the isotropic, partially debonded one so that Eshelby's solution of a perfectly bonded inclusion could be used. [Eshelby, J. D. (1957). The determination of the elastic field of an ellipsoidal inclusion, and related problems. *Proc. R. Soc. London* **A241**, 376–396]. Two types of debonding configuration are considered: the first type occurs on the top and bottom of the oblate inclusions and the second one exists on the lateral surface of the prolate inclusions. Albeit approximate, the method is simple and capable of providing explicit results for the five independent moduli in terms of the volume concentrations and aspect ratio of the partially-debonded and perfectly-bonded inclusions. The results are given for the spherical and various inclusion shapes. It is shown that, with spherical inclusions, the longitudinal Young's modulus E_{11} and axial shear modulus μ_{12} in type 1, and the transverse Young's modulus E_{22}, plane-strain bulk modulus k_{23}, and the axial and transverse shear moduli in type 2, can all be greatly affected by partial debonding. Examination on the influence of inclusion shape indicates that disc-shaped inclusions in the first type and prolate ones is the second type lead to stronger moduli reduction than spheres. Copyright © 1996 Elsevier Science Ltd.

1. INTRODUCTION

This paper is concerned with the determination of the effective elastic behavior of two partially debonded composites. When a particle-reinforced composite is subjected to a uniaxial tension, interfacial debonding on the top and bottom of the interface may take place, but when the system is subjected to a transverse biaxial tension interfacial debonding may take place on the lateral surface. The debonded inclusion will lose its load-carrying capacity in the debonded direction, but as it remains perfectly bonded in the other directions it is still capable of transmitting stress to the matrix. While with homogeneously dispersed, perfectly-bonded spherical particles, the overall system is isotropic, it becomes transversely isotropic after either of such partial debondings. This is necessarily so with aligned spheroidal inclusions. Our objective here is to derive the five transversely isotropic effective moduli for both types of partial debonding.

A schematic diagram of such an idealized system is shown in Fig. 1(a) for the first type and in Fig. 1(b) for the second one, where the symmetric direction of the spheroidal inclusions is identified as direction 1. The matrix and inclusions are referred to as phase 0 and 1, respectively, and the volume concentration of the r-th phase is denoted by c_r ($c_0+c_1=1$). We further divide the inclusions into two groups: the perfectly-bonded particles and the partially debonded—or damaged—ones, and denote their respective volume concentrations by c_p and c_d ($c_p+c_d=c_1$). For simplicity both phases will be taken to be isotropic, so that the elastic moduli tensor of the r-th phase L_r, can be represented by its bulk and shear moduli as

† Visiting Scholar, from Department of Civil Engineering, Shenyang Architectural Engineering Institute, Shenyang, Liaoning, People's Republic of China.

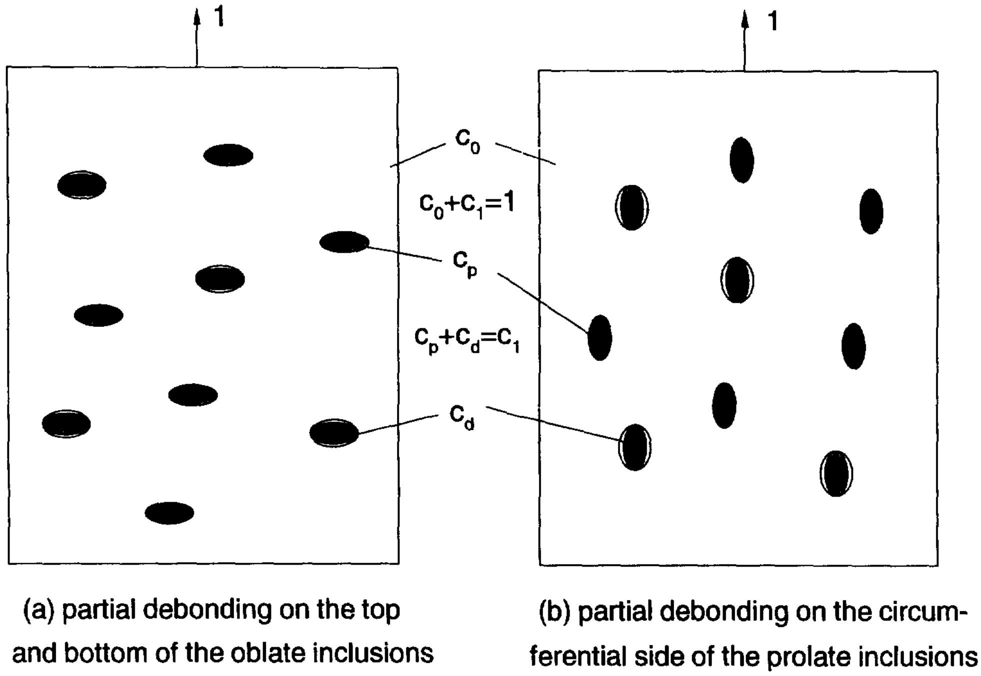

Fig. 1. Schematic diagram of a hybrid composite with two types of partial debonding.

$$L_r = (3\kappa_r, 2\mu_r), \tag{1.1}$$

in Hill's (1965) short-hand format. The corresponding Young's modulus and Poisson's ratio are denoted by E_r and ν_r.

While spherical inclusions represent the most common particle shape, inclusions of the oblate and prolate shapes aligned along direction 1 are also of some fundamental interest. However, to meet the requirement in the present model that a partially debonded particle will lose its tensile load-carrying capacity along the debonded direction, the prolate shape should be excluded from consideration in the first type and the oblate shape be excluded in the second one. This is in light of the fact that such a partially-debonded inclusion may still carry significant axial tensile stress in the first type, especially so when the inclusions take the shape of a long needle. This is equally so for the second type when the inclusions become very flat. Thus we shall give a detailed examination for spherical particles first, and then consider the problem for only aligned oblate inclusions for the first type, and aligned prolate inclusions for the second one. The focus there will be on the influence of aspect ratio α (the thickness-to-diameter ratio) of the spheroidal inclusions on the transversely isotropic moduli of the partially debonded system.

Other types of interfacial damage may also affect the overall moduli. For instance with sliding inclusions Jasiuk *et al.* (1987) and Shibata *et al.* (1990) have found that the effective shear modulus can be greatly reduced by such a process.

2. A FICTITIOUS TRANSVERSELY ISOTROPIC INCLUSION AND THE EFFECTIVE MODULI OF THE PARTIALLY DEBONDED COMPOSITE

Effective elastic moduli of a perfectly bonded composite can be examined by various micromechanical models; a discussion and comparison among the three widely used ones—Mori and Tanaka's (1973) method (M-T), the differential scheme (DS), and Christensen and Lo's (1979) generalized self-consistent model (GSC)—can be found in Christensen (1990) for the cases of spherical particles and aligned circular fibers. Christensen pushed the comparison to the very high concentration range for the transverse shear property with rigid inclusions, for both compressible and incompressible matrix. His primary findings for the transverse shear modulus are: (i) the GSC is the most accurate one among the three,

(ii) with compressible matrix M-T provides a result very close to that of GSC whereas DS leads to a substantially stiffer response, and (iii) with an incompressible matrix DS is too soft and M-T is even softer. For the bulk modulus it is well known that both GSC and M-T coincide, while the estimate by DS remains too stiff.

Due to its versatility that the inclusion shape can be accounted for explicitly, the Mori-Tanaka method will be used here, but for the transverse shear property it must be restricted to a compressible matrix. However for the present problem, as the inclusion-matrix interface for the debonded regions is not perfectly bonded, Eshelby's (1957) solution can not be applied directly in Mori-Tanaka's approach. To circumvent this difficulty, we note that, for the first type of debonding configuration the debonded regions on the top and bottom of the inclusion can not transfer both tensile and shear stress (in an average sense), and therefore if the isotropic debonded inclusion is replaced by a fictitious transversely isotropic one with a property that its average tensile stress σ_{11} and shear stresses σ_{12} and σ_{13} will always be zero, then this fictitious inclusion can be treated as an ordinary bonded inclusion. Similar argument can be made on the lateral surface for the second type, but in both cases a new transversely isotropic elastic property must be assigned to the fictitious inclusion.

In dealing with a transversely isotropic material, such as this newly introduced inclusion or the overall, partially debonded composite, it is convenient to use Hill's (1964) stress-strain relations

$$
\begin{aligned}
\tfrac{1}{2}(\sigma_{22}+\sigma_{33}) &= k(\varepsilon_{22}+\varepsilon_{33})+l'\varepsilon_{11},\\
\sigma_{11} &= l(\varepsilon_{22}+\varepsilon_{33})+n\varepsilon_{11},\\
\sigma_{22}-\sigma_{33} &= 2m(\varepsilon_{22}-\varepsilon_{33}), \quad \sigma_{23} = 2m\varepsilon_{23},\\
\sigma_{12} &= 2p\varepsilon_{12}, \quad \sigma_{13} = 2p\varepsilon_{13},
\end{aligned}
\tag{1}
$$

where direction 1 is symmetric and plane 2-3 isotropic. Then, in Walpole's (1969) short-hand notations, the transversely isotropic elastic moduli tensor can be written as

$$
L = (2k, l, l', n, 2m, 2p). \tag{2}
$$

Since tensor L is diagonally symmetric ($l = l'$), it can be further shortened to

$$
L = (2k, l, n, 2m, 2p). \tag{3}
$$

When the system is isotropic, it reduces to

$$
L = (2k, k-\mu, k+\mu, 2\mu, 2\mu), \tag{4}
$$

where k is the plane-strain bulk modulus ($k = \kappa+\mu/3$).

2.1. *Debonding on the top and bottom of the oblate inclusions* ($\alpha \leqslant 1$)

In order to find the five elastic moduli for the fictitious, transversely isotropic inclusion, we first return to the isotropic, debonded inclusion, with the moduli cast in the form of (4) but with a subscript 1. Since $\sigma_{11} = 0$, one has

$$
\begin{aligned}
\varepsilon_{11} &= -\frac{k_1-\mu_1}{k_1+\mu_1}(\varepsilon_{22}+\varepsilon_{33}),\\
\tfrac{1}{2}(\sigma_{22}+\sigma_{33}) &= \frac{\mu_1(3k_1-\mu_1)}{k_1+\mu_1}(\varepsilon_{22}+\varepsilon_{33}).
\end{aligned}
\tag{5}
$$

To ensure the equivalence between the original, partially debonded isotropic inclusion and the fictitious, perfectly bonded transversely isotropic inclusion, the elastic moduli of this inclusion, to be denoted by

$$L_2 = (2k_2, l_2, n_2, 2m_2, 2p_2), \tag{6}$$

must satisfy

$$l_2 = 0, \quad n_2 = 0,$$
$$k_2 = \frac{\mu_1(3k_1 - \mu_1)}{k_1 + \mu_1},$$
$$m_2 = \mu_1, \quad p_2 = 0, \tag{7}$$

which further implies that its tensile Young's modulus $E_{11}^{(2)} = 0$ and its transverse Young's modulus $E_{22}^{(2)} = E_1$.

2.2. *Debonding on the lateral surface of the prolate inclusions* ($\alpha \geqslant 1$)

In this case debonding takes place on the lateral 2-3 surface so that $\sigma_{22} = \sigma_{33} = 0$. It follows that

$$\varepsilon_{22} + \varepsilon_{33} = -\frac{l_1}{k_1}\varepsilon_{11},$$
$$\sigma_{11} = \frac{\mu_1(3k_1 - \mu_1)}{k_1}\varepsilon_{11}. \tag{8}$$

Furthermore, the aligned prolate inclusions also carry no shear stress, $\sigma_{12} = \sigma_{23} = 0$. Thus, the five components of the moduli of the fictitious transversely isotropic inclusion are

$$n_2 = \frac{\mu_1(3k_1 - \mu_1)}{k_1} = E_1,$$
$$k_2 = l_2 = 0, \quad m_2 = p_2 = 0, \tag{9}$$

which also implies that its longitudinal $E_{11}^{(2)} = E_1$ and transverse $E_{22}^{(2)} = 0$.

For both types of partial debonding the problem now reduces to a hybrid composite containing two kinds of identically shaped inclusions, one being isotropic and the other transversely isotropic. The M-T moduli tensor for this class of composite has be derived by Weng (1990), as

$$L = (\Sigma c_r L_r A_r)(\Sigma c_r A_r)^{-1}, \tag{10}$$

in symbolic notations, where the summation Σ is extended to all three phases, and, in term of Eshelby's S-tensor

$$A_r = [I + SL_0^{-1}(L_r - L_0)]^{-1}, \tag{11}$$

which is the strain concentration tensor of an ellipsoidal inclusion embedded in an infinitely extended matrix. The inner product of two tensors here is given as $LA = L_{ijkl}A_{klmn}$. This effective moduli tensor satisfies the diagonal symmetry ($l = l'$) and, as proved by Weng (1992), it always lies on or inside Willis' bounds (1977).

All the tensors in (10) and (11) can be cast in the transversely isotropic form as in (1) and (2), and for the S-tensor, it is

$$S = (S_{2222} + S_{2233}, S_{1122}, S_{2211}, S_{1111}, 2S_{2323}, 2S_{1212}), \tag{12}$$

noting that $S_{1122} \neq S_{2211}$, unless the inclusion becomes spherical. The inner products and inverse of the transversely isotropic tensors also result in a transversely isotropic tensor;

its six components—in the form of (2)—can be readily evaluated following Walpole's (1981) procedure. It follows that the five effective elastic moduli are given by

$$
\begin{aligned}
k = {} & [\{k_0[S_{1111}(S_{2222}+S_{2233}-1)-2S_{1122}S_{2211}]+(k_0-\mu_0)S_{1122}\}(a_1a_4-2a_2a_3) \\
& +k_0[1+(S_{2222}+S_{2233}-1)a_1+S_{1111}a_4+2(S_{1122}a_3+S_{2211}a_2)] \\
& -(k_0-\mu_0)a_2]/a, \\
l = {} & [\{(k_0-\mu_0)[S_{1111}(S_{2222}+S_{2233}-1)-2S_{1122}S_{2211}]+(k_0+\mu_0)S_{1122}\} \\
& \times(a_1a_4-2a_2a_3)+(k_0-\mu_0)[(S_{2222}+S_{2233}-1)a_1+2S_{1122}a_3+2S_{2211}a_2 \\
& +S_{1111}a_4+1]-(k_0+\mu_0)a_2] \\
n = {} & [\{(k_0+\mu_0)[(S_{1111}-1)(S_{2222}+S_{2233})-2S_{1122}S_{2211}]+2(k_0-\mu_0)S_{2211}\} \\
& \times(a_1a_4-2a_2a_3)+(k_0+\mu_0)[(S_{1111}-1)a_4+2S_{1122}a_3+2S_{2211}a_2 \\
& +(S_{2222}+S_{2233})a_1+1]-2(k_0-\mu_0)a_3]/a, \\
m = {} & \mu_0\left(1-\frac{a_5}{1+2S_{2323}a_5}\right), \\
p = {} & \mu_0\left(1-\frac{a_6}{1+2S_{1212}a_6}\right),
\end{aligned}
\tag{13}
$$

where

$$
\begin{aligned}
a = {} & [S_{1111}(S_{2222}+S_{2233})-2S_{1122}S_{2211}](a_1a_4-2a_2a_3)+[(S_{2222}+S_{2233})a_1 \\
& +S_{1111}a_4+2S_{1122}a_3+2S_{2211}a_2+1],
\end{aligned}
\tag{14}
$$

for both types of debonding sketched in Fig. 1. The constants $a_1 \ldots a_6$, however, are different, and are given in the Appendix. The tensile Young's modulus E_{11}, major Poisson's ratio ν_{12} and transverse Young's modulus $E_{22}(=E_{33})$ are in turn given by

$$
\begin{aligned}
E_{11} &= n-l^2/k, \quad \nu_{12} = l/2k, \\
E_{22} &= \frac{4k_{23}}{k_{23}/\mu_{23}+1+4\nu_{12}^2k_{23}/E_{11}},
\end{aligned}
\tag{15}
$$

with the engineering constants $k_{23}=k$, $\mu_{23}=m$, and $\mu_{12}=p$.

We note in passing that, in order to apply the Eshelby-Mori-Tanaka theory to the present problem, replacement of the partially debonded isotropic inclusions by a perfectly bonded, transversely isotropic inclusion is a necessary step. If one were to invoke the condition $\sigma_{11}=0$ in the first type (or $\sigma_{22}=\sigma_{33}=0$ in the second one) and still keep all the isotropic constants for the debonded inclusion in the 2 and 3 directions (or 1-direction in the second type), the derived overall moduli tensor would become asymmetric.

3. SPHERICAL INCLUSIONS

The preceding results can be simplified for spherical inclusions by invoking the values of S-tensor. After some lengthy algebra, we arrive at

$$
\begin{aligned}
k = {} & k_0\{(1+\nu_0)(1-2\nu_0)(13-15\nu_0)(a_1a_4-2a_2a_3)+3(1-\nu_0)[3(3-5\nu_0)a_1 \\
& -(7-5\nu_0)a_4+2(1-5\nu_0)a_3-2(15\nu_0^2-10\nu_0-1)a_2-15(1-\nu_0)]\}/a, \\
l = {} & 2k_0\{(1+\nu_0)(1-2\nu_0)(3-5\nu_0)(a_1a_4-2a_2a_3)+3(1-\nu_0)[3(3-5\nu_0)\nu_0a_1
\end{aligned}
$$

$$-(7-5\nu_0)\nu_0 a_4+2(1-5\nu_0)\nu_0 a_3+(5-\nu_0)(3-5\nu_0)a_2-15(1-\nu_0)\nu_0]\}/a,$$

$$n = -2k_0(1-\nu_0)\{-10(1+\nu_0)(1-2\nu_0)(a_1a_4-2a_2a_3)+3(1-\nu_0)[6a_1 -2(4-5\nu_0)a_4-2(1+10\nu_0)a_3-2(1-5\nu_0)a_2+15(1-\nu_0)]\}/a,$$

$$m = \mu_0\left[1-\frac{a_5}{1+2a_5(4-5\nu_0)/(1-\nu_0)/15}\right],$$

$$p = \mu_0\left[1-\frac{a_6}{1+2a_6(4-5\nu_0)/(1-\nu_0)/15}\right], \tag{16}$$

where

$$a = -2(1+\nu_0)(4-5\nu_0)(a_1a_4-2a_2a_3)+3(1-\nu_0)[-6a_1-(7-5\nu_0)a_4 +2(1-5\nu_0)(a_2+a_3)-15(1-\nu_0)], \tag{17}$$

and $a_1, \ldots a_6$ are also given in the Appendix.

In the above equations, both perfectly bonded and partially debonded inclusions coexist, and they apply to both types of debonding configuration in Fig. 1. These two configurations are now considered separately.

3.1. *Debonding on the top and bottom of the spherical inclusions* ($\alpha = 1$)

First we simply these results for the important case when all inclusions are in the partially-debonded state ($c_d = c_1, c_p = 0$):

$$E_{11} = 2E_0c_0\left\{12\frac{E_1}{1-\nu_1}-(7-5\nu_0)\left[\frac{E_1}{1-\nu_1}-\frac{E_0}{1-\nu_0}\right]\right\}\Big/ \left\{(13-15\nu_0)(1+\nu_0)c_0^2\left[\frac{E_1}{1-\nu_1}-\frac{E_0}{1-\nu_0}\right]+3[15(1-\nu_0) -4(4-5\nu_0)c_0]\frac{E_1}{1-\nu_1}(1+\nu_0)+3(9+5\nu_0)(1-\nu_0)c_0\frac{E_0}{1-\nu_0}\right\},$$

$$k_{23} = E_0\left\{(13-15\nu_0)(1+\nu_0)c_0^2\left[\frac{E_1}{1-\nu_1}-\frac{E_0}{1-\nu_0}\right]+3[15(1-\nu_0) -4(4-5\nu_0)c_0]\frac{E_1}{1-\nu_1}(1+\nu_0)+3(9+5\nu_0)(1-\nu_0)c_0\frac{E_0}{1-\nu_0}\right\}\Big/ 2(1+\nu_0)\left\{-2(1+\nu_0)(4-5\nu_0)c_0^2\left[\frac{E_1}{1-\nu_1}-\frac{E_0}{1-\nu_0}\right]-(1-\nu_0) \times[3(13-5\nu_0)c_0-45(1-\nu_0)]\frac{E_0}{1-\nu_0}+6(1+\nu_0)(3-5\nu_0)c_0\frac{E_1}{1-\nu_1}\right\},$$

$$\nu_{12} = \left\{(1+\nu_0)(3-5\nu_0)c_1\left[\frac{E_1}{1-\nu_1}-\frac{E_0}{1-\nu_0}\right] +3\left[(1-\nu_0)(1+5\nu_0)\frac{E_0}{1-\nu_0}-(1+\nu_0)(1-5\nu_0)\frac{E_1}{1-\nu_1}\right]\right\}c_0\Big/ \left\{(13-15\nu_0)(1+\nu_0)c_0^2\left[\frac{E_1}{1-\nu_1}-\frac{E_0}{1-\nu_0}\right]+3[15(1-\nu_0)\right.$$

$$-4(4-5\nu_0)c_0]\frac{E_1}{1-\nu_1}(1+\nu_0)+3(9+5\nu_0)(1-\nu_0)c_0\frac{E_0}{1-\nu_0}\bigg\},$$

$$\mu_{23}=\mu_0\frac{15(1-\nu_0)\mu_0-(7-5\nu_0)c_0(\mu_1-\mu_0)}{2(4-5\nu_0)c_0(\mu_1-\mu_0)+15(1-\nu_0)\mu_0},$$

$$\mu_{12}=\mu_0/\left[1+15\frac{c_1}{c_0}\frac{1-\nu_0}{7-5\nu_0}\right], \tag{18}$$

with E_{22} given by (15), if needed.

At this point it is appropriate to point out that Taya (1981) was probably the first to use Mori-Tanaka's method to address the first type of the partially debonded problem, but only for rigid inclusions. This early study was concerned with the void growth at the interface of rigid particles in a Newtonian matrix. As the inclusion was rigid he further made use of the condition $\varepsilon_{22}=\varepsilon_{33}=0$ in the transverse directions. Subsequently, Mochida *et al.* (1991) also used this approach to find the longitudinal Young's modulus E_{11} of the hybrid composite containing spherical inclusions, but in the process they treated the debonded elastic inclusions as rigid particles while maintaining the perfectly bonded inclusions to be elastic. Consideration of rigid inclusions can greatly simplify the problem, as in the case $\varepsilon_{22}=\varepsilon_{33}=0$ and there is no need to introduce a fictitious transversely isotropic inclusion to replace the isotropic one. The idealization of a debonded *elastic* inclusion by a *rigid* one, however, is bound to cause an error; such an error largely depends on the elastic modular ratio of the inclusions to the matrix. For instance, assuming both $\nu_1=\nu_0=1/3$ and a total inclusion concentration of $c_1=0.2$, the normalized E_{11}/E_0 for the hybrid composite as calculated by the present theory and their method are shown in Fig. 2, as a function of c_d at five selected E_1/E_0 ratios. When the inclusions are indeed rigid, both approaches coincide with each other. In general their approximation is reasonable in the region of high E_1/E_0 and low c_d, but at low E_1/E_0 and high c_d it must be used with caution.

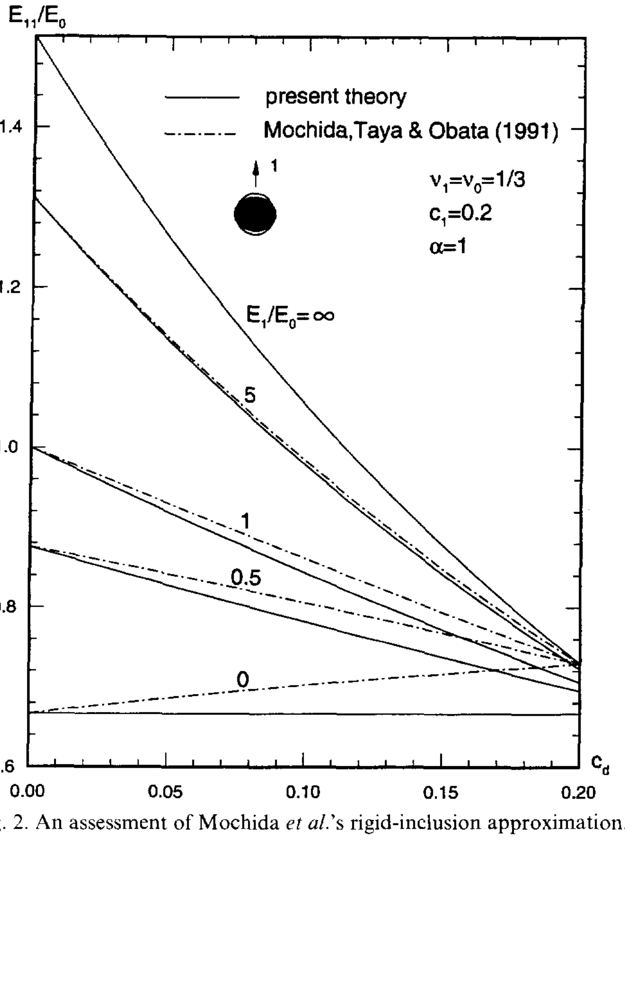

Fig. 2. An assessment of Mochida *et al.*'s rigid-inclusion approximation.

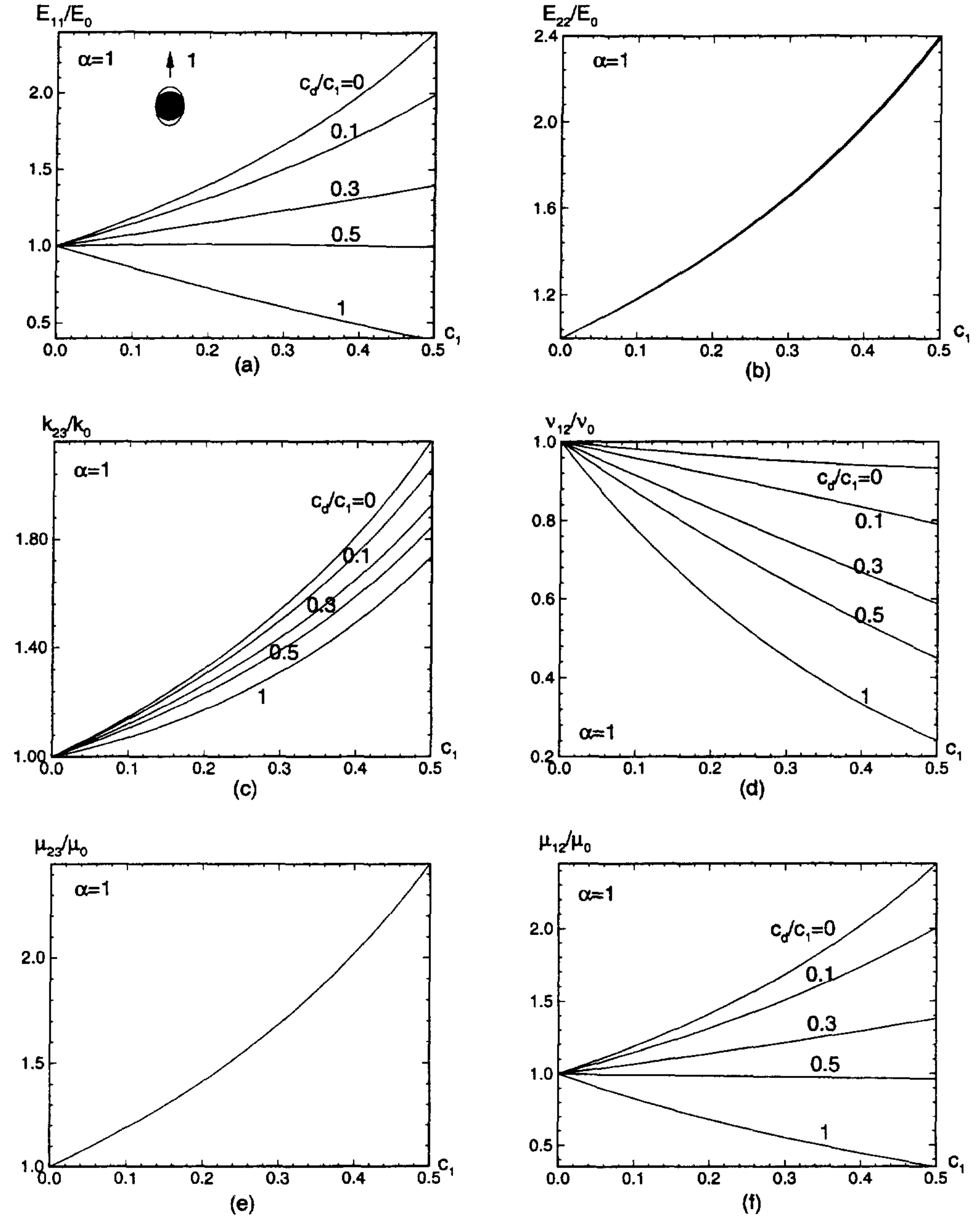

Fig. 3. The transversely isotropic moduli of a hybrid composite containing spherical inclusions partially debonded on the top and bottom.

We now examine the influence of volume concentration c_d of the partially debonded particles on the five transversely isotropic effective moduli E_{11}, E_{22}, k_{23}, μ_{23}, μ_{12}, and the major Poisson's ratio ν_{12}. The calculations were based on the properties of $E_1 = 10E_0$ and $\nu_1 = \nu_0 = 1/3$, and the results are shown in Fig. 3 (a)–(f). In each figure five selected ratios of c_d/c_1 have been considered, such that $c_d/c_1 = 0$ corresponds to the ordinary two-phase composite with perfect bonding and $c_d/c_1 = 1$ refers to a two-phase system with only partially debonded particles. For E_{11}, the total inclusions would continue to strengthen the system even with 30% of the total particles in the partially debonded state, but as the fraction increases beyond 50% the system will weaken. Such is also the case with μ_{12}. The moduli E_{22} and μ_{23} are totally insensitive to partial debonding. The plane-strain bulk modulus also increases with increasing c_1 regardless of the c_d/c_1 ratio, but this ratio now plays a clearly discernible role.

3.2. *Debonding on the lateral surface of the spherical inclusions* ($\alpha = 1$)

When all the inclusions are in the partially debonded state ($c_d = c_1, c_p = 0$), equations (15) and (16) can be simplified to yield the following five effective engineering moduli:

$$E_{11} = E_0c_0[5(1-\nu_0)(4-4\nu_0-5\nu_0^2)E_1-3(3-5\nu_0)(E_1-E_0)]/$$
$$\{[6+5(1-\nu_0^2)(1-5\nu_0)](E_1-E_0)c_0+5(1-\nu_0)(4-4\nu_0-5\nu_0^2)E_0\},$$
$$k_{23} = k_0c_0\{[6+5(1-\nu_0^2)(1-5\nu_0)](E_1-E_0)c_0+5(1-\nu_0)(4-4\nu_0-5\nu_0^2)E_0\}/$$
$$\{3(3-5\nu_0)(E_1-E_0)c_0^2-\tfrac{75}{2}(1-\nu_0)^2E_0c_1-5(1-\nu_0)(4-4\nu_0-5\nu_0^2)E_1c_0\},$$
$$\nu_{12} = \{[5(1-\nu_0^2)-(13-25\nu_0^2)\nu_0](E_1-E_0)c_0+5(1-\nu_0)[(1+2\nu_0-5\nu_0^2)E_0$$
$$-(1+\nu_0)(1-2\nu_0)(1-5\nu_0)E_1]\}/\{[6+5(1-\nu_0^2)(1-5\nu_0)](E_1-E_0)c_0$$
$$+5(1-\nu_0)(4-4\nu_0-5\nu_0^2)E_0\},$$
$$\mu_{23} = \mu_{12} = \mu_0\frac{(7-5\nu_0)c_0}{(7-5\nu_0)+2c_1(4-5\nu_0)}. \qquad (19)$$

Returning to the hybrid composite at the same five selected c_d/c_1 ratios, the effective moduli are given in Fig. 4. As debonding now occurs on the 2-3 lateral surface, E_{22}, k_{23}, μ_{23} and μ_{12} are all visibly affected by an increasing c_d/c_1 ratio. The longitudinal Young's modulus E_{11}—similar to E_{22} in Fig. 3—is the sole quantity not disturbed by this partial debonding.

To place the influence of both types of *partial* debonding in proper perspective, we plot in Fig. 5 the effective moduli of the two-phase composite under the four bonding conditions: (a) perfect bonding, (b) partial debonding on the top and bottom, (c) partial debonding on the lateral surface, and (d) complete debonding, with no perfectly bonded particles in (b) and (c). The moduli given in Fig. 5 (a), except for ν_{12}, all increase with increasing particle concentration, whereas those in Fig. 5 (d) all decrease, as expected. As the system is isotropic in both cases, these five components also satisfy the usual isotropic connections. The results for both types of partial debonding are seen to lie between the two. In Fig. 5 (b) both E_{11} and μ_{12} decrease with increasing debonding, with μ_{23}, E_{22} and k_{23} still exhibiting the stiffening effect, and in Fig. 5 (c) all the three transverse moduli are seen to decrease, with only E_{11} showing a strengthening effect.

4. THE INFLUENCE OF INCLUSION SHAPE α ON THE EFFECTIVE MODULI

4.1. *Debonding on the top and bottom of the oblate inclusions* ($\alpha \leqslant 1$)

The influence of inclusion shape—or the aspect ratio α of the oblate inclusions—is shown in Fig. 6. In each curve four selected shapes have been studied, ranging from spheres to thin discs with $\alpha = 0.1$. This set of results has been calculated from (13), again using the properties $E_1/E_0 = 10$ and $\nu_1 = \nu_0 = 1/3$. All are under a total inclusion concentration of $c_1 = 0.2$, with the debonded portion again represented by c_d. The condition $c_d = 0$ corresponds to the perfectly bonded two-phase composite, and as c_d increases from 0 to 0.2, each of these five moduli also decreases. The reduction is most dramatic in E_{11}, k_{23} and μ_{12}, and for E_{11} and μ_{12} disc-shaped inclusions are seen to cause a more pronounced weakening effect. The influence of c_d on E_{22} and μ_{23} is not visible and the debonded inclusions can be effectively treated as perfectly bonded ones. For these moduli discs provide a stronger reinforcement than spheres.

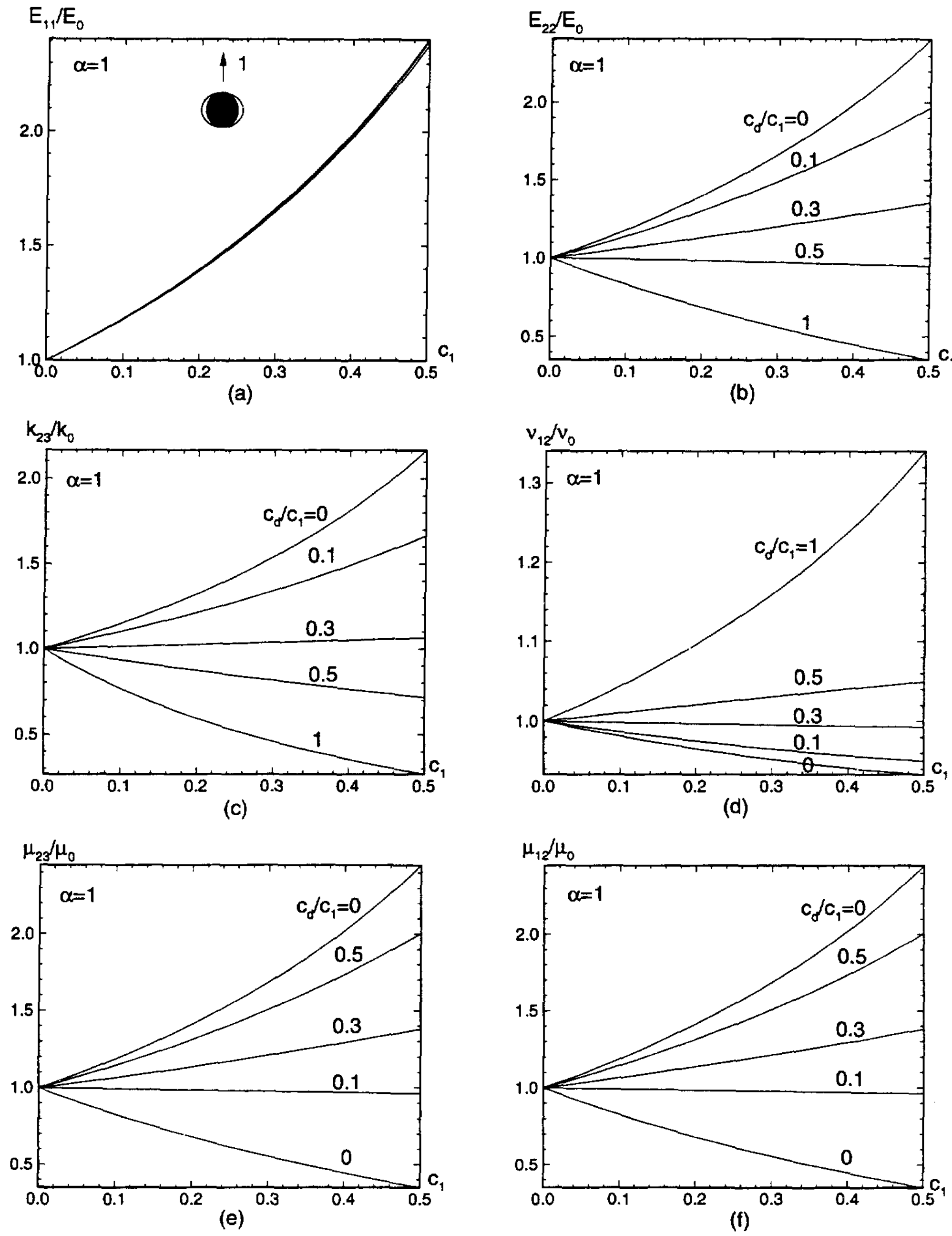

Fig. 4. The transversely isotropic moduli of a hybrid composite containing spherical inclusions partially debonded on the circumferential side.

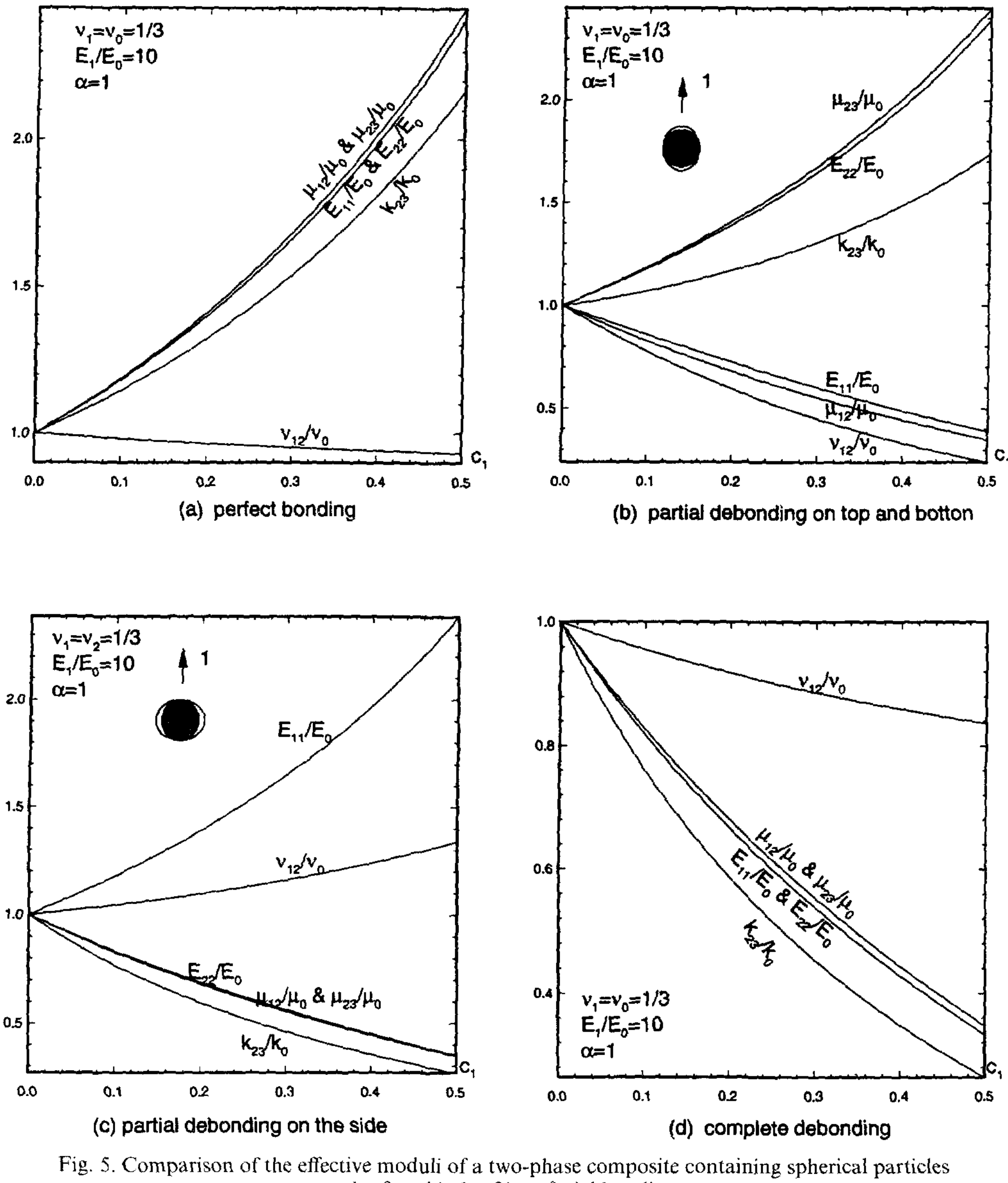

Fig. 5. Comparison of the effective moduli of a two-phase composite containing spherical particles under four kinds of interfacial bonding.

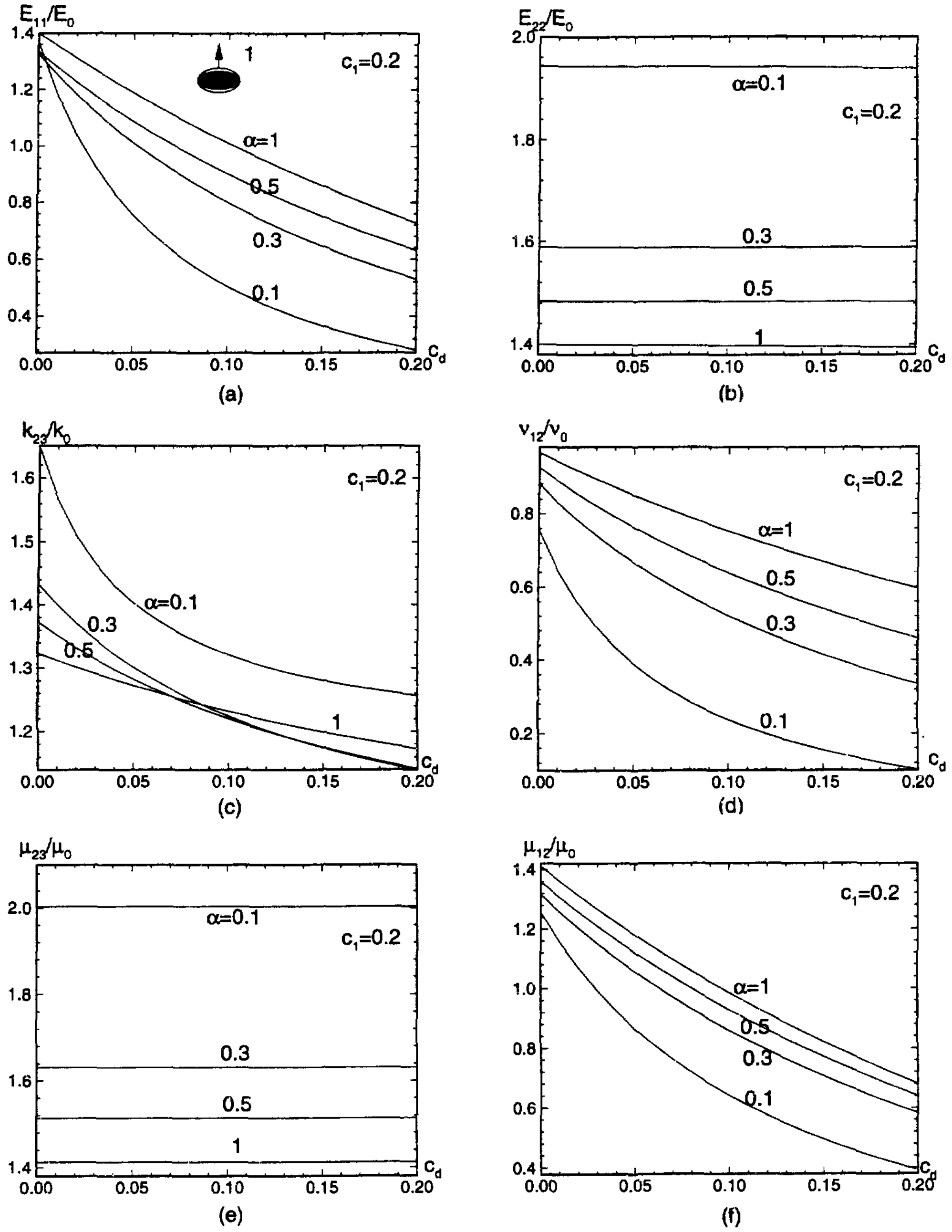

Fig. 6. Influence of inclusion shape on the transversely isotropic moduli of a hybrid composite containing oblate inclusions partially debonded on the top and bottom.

4.2. *Debonding on the lateral surface of the prolate inclusions* ($\alpha \geqslant 1$)

In this case the four selected inclusion shapes are $\alpha = 1, 2, 3$ and 5 and the results are given in Fig. 7. Consistent with the results of spherical inclusions, the four transverse moduli all suffer a visible reduction as c_d increases. Prolate-shaped inclusions also lead to a greater reduction in these effective moduli than the spherical ones. The only modulus not affected in any significant way is E_{11}, for which prolate inclusions with a greater aspect ratio also give rise to a stiffer response.

Acknowledgements—This work was supported by the National Science Foundation, under Grant MSS-9114745, and by the Office of Naval Research, under Grant N-00014-91-J1937. Dr Yapa Rajapakse was the Program Manager at ONR. The support of the Pittsburgh Supercomputer Center is also gratefully acknowledged.

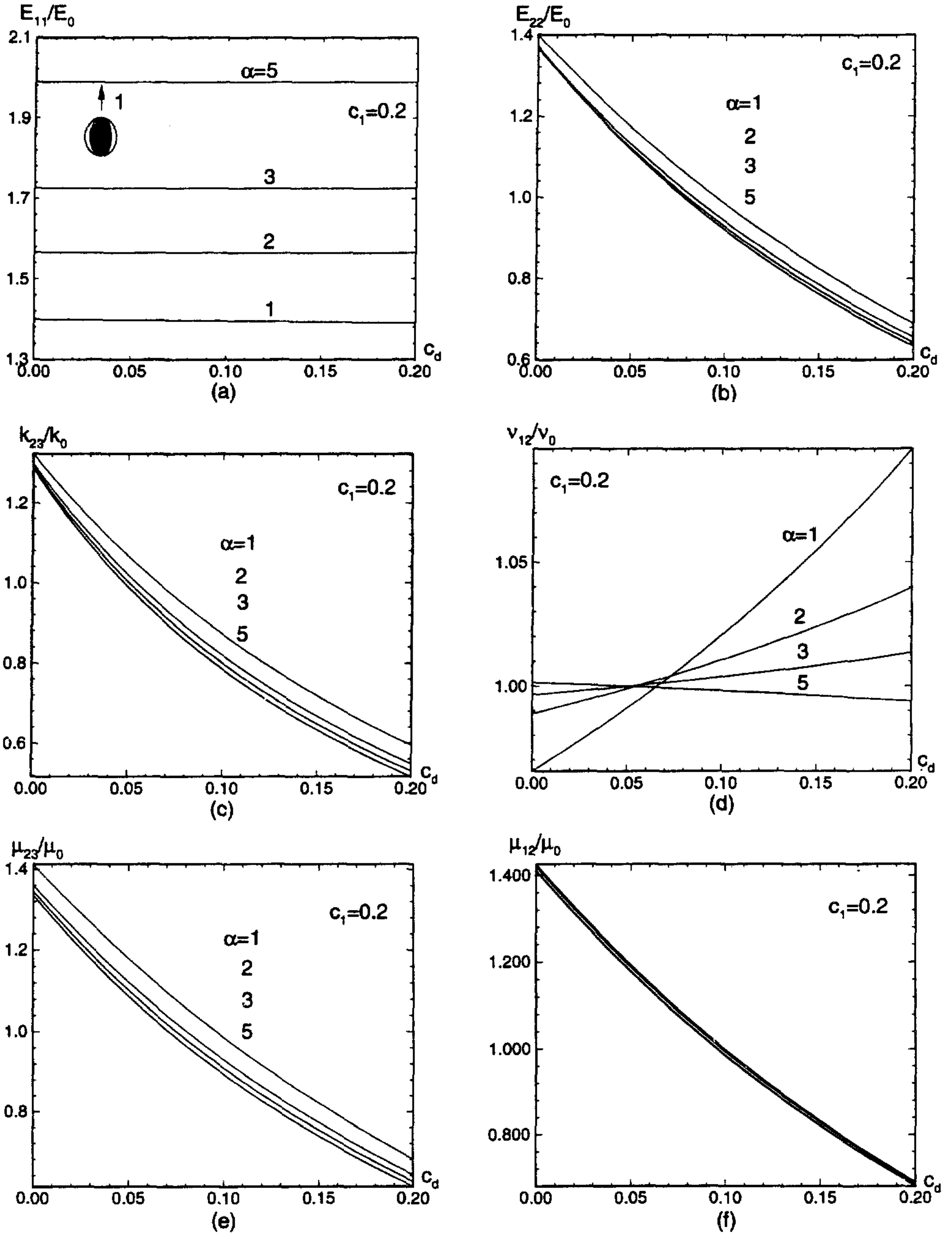

Fig. 7. Influence of inclusion shape on the transversely isotropic moduli of a hybrid composite containing prolate inclusions partially debonded on the circumferential side.

REFERENCES

Christensen, R. M. and Lo, K. H. (1979). Solutions for effective shear properties in three phase sphere and cylinder models. *J. Mech. Phys. Solids* **27**, 315–330.

Christensen, R. M. (1990). A critical evaluation for a class of micromechanics models. *J. Mech. Phys. Solids* **38**, 379–404.

Eshelby, J. D. (1957). The determination of the elastic field of an ellipsoidal inclusion, and related problems. *Proc. R. Soc. London* **A241**, 376–396.

Hill, R. (1964). Theory of mechanical properties of fiber-strengthened materials: I. Elastic behavior. *J. Mech. Phys. Solids* **12**, 199–212.

Hill, R. (1965). Continuum micromechanics of elastoplastic polycrystals. *J. Mech. Phys. Solids* **13**, 89–101.

Jasiuk, I., Tsuchida, E. and Mura, T. (1987). The sliding inclusion under shear. *Int. J. Solids Struct.* **23**, 1373–1385.

Mochida, T., Taya, M. and Obata, M. (1991). Effect of damaged particles on the stiffness of a particle/metal matrix composite. *JSME Int. J.* **34**, 187–193.

Mori, T. and Tanaka, K. (1973). Average stress in matrix and average elastic energy of materials with misfitting inclusions. *Acta Metall.* **21,** 571–574.

Shibata, S., Jasiuk, I., Mori, T. and Mura, T. (1990). Successive iteration method applied to a composite containing sliding inclusions: overall elastic constants. In *Proc. Japan-US CCM-V* (ed. A. Kobayashi), Tokyo.

Taya, M. (1981). Growth of a debonded void at a rigid secondary particle in a viscous metal. In *Advances in Aerospace Structures and Materials* (eds S. S. Wang and W. J. Renton), ASME AD-01, 229–304, New York.

Walpole, L. J. (1969). On the overall elastic moduli of composite materials. *J. Mech. Phys. Solids* **17,** 235–251.

Walpole, L. J. (1981). Elastic behavior of composite materials: theoretical foundations. *Adv. Appl. Mech.* **21,** 169–242.

Weng, G. J. (1984). Some elastic properties of reinforced solids, with special reference to isotropic ones containing spherical inclusions. *Int. J. Engng Sci.* **22,** 845–856.

Weng, G. J. (1990). The theoretical connection between Mori-Tanaka's theory and the Hashin-Shtrikman-Walpole bounds. *Int. J. Engng Sci.* **28,** 1111–1120.

Weng, G. J. (1992). Explicit evaluation of Willis' bounds with ellipsoidal inclusions. *Int. J. Engng Sci.* **30,** 83–92.

Willis, J. R., (1977). Bounds and self-consistent estimates for the overall properties of anisotropic composites. *J. Mech. Phys. Solids* **25,** 185–202.

APPENDIX: CONSTANTS $a_1 \ldots a_6$ IN (13) AND (16)

These constants are given by

$$\begin{aligned} a_1 &= c_p c_1 + c_d c_2, \quad a_2 = c_p g_1 + c_d g_2, \\ a_3 &= c_p h_1 + c_d h_2, \quad a_4 = c_p d_1 + c_d d_2, \\ a_5 &= c_p e_1 + c_d e_2, \quad a_6 = c_p f_1 + c_d f_2, \end{aligned} \tag{A.1}$$

where c_p and c_d are the volume concentrations of the perfectly bonded and partially debonded inclusions, respectively. In this equation

$$\begin{aligned} c_1 &= \{-2[3(k_1-k_0)-(\mu_1-\mu_0)](\mu_1-\mu_0)S_{1111}+2(3k_0-\mu_0)\mu_0 \\ &\quad -2(k_1\mu_0+k_0\mu_1)-2(k_1-\mu_1)\mu_0\}/b_1, \\ g_1 &= \{2[3(k_1-k_0)-(\mu_1-\mu_0)](\mu_1-\mu_0)S_{1122}-2(k_1\mu_0-k_0\mu_1)\}/b_1, \\ h_1 &= \{2[3(k_1-k_0)-(\mu_1-\mu_0)](\mu_1-\mu_0)S_{2211}-2(k_1\mu_0-k_0\mu_1)\}/b_1, \\ d_1 &= \{-2[3(k_1-k_0)-(\mu_1-\mu_0)](\mu_1-\mu_0)(S_{2222}+S_{2233})+2(3k_0-\mu_0)\mu_0 \\ &\quad -2(k_1\mu_0+k_0\mu_1)-2\mu_1(k_0-\mu_0)\}/b_1, \\ e_1 &= -1/\left(2S_{2323}+\frac{\mu_0}{\mu_1-\mu_0}\right), \\ f_1 &= -1/\left(2S_{1212}+\frac{\mu_0}{\mu_1-\mu_0}\right), \\ b_1 &= 2[S_{1111}(S_{2222}+S_{2233})-2S_{1122}S_{2211}][3(k_1-k_0)-(\mu_1-\mu_0)](\mu_1-\mu_0) \\ &\quad +2(1-S_{1111}-S_{2222}-S_{2233})(3k_0-\mu_0)\mu_0 \\ &\quad +2(S_{1111}+S_{2222}+S_{2233})(k_1\mu_0+k_0\mu_1)+4(S_{1122}+S_{2211})(k_1\mu_0-k_0\mu_1) \\ &\quad +(S_{2222}+S_{2233})(k_1-\mu_1)\mu_0+2S_{1111}\mu_1(k_0-\mu_0), \end{aligned} \tag{A.2}$$

which are associated with the perfectly bonded inclusions and, for the type-1 debonding in Fig. 1(a)

$$\begin{aligned} c_2 &= \{2[(3k_0-\mu_0)\mu_0-k_2(k_0+\mu_0)](1-S_{1111})\}/b_2, \\ g_2 &= \{2[(3k_0-\mu_0)\mu_0-k_2(k_0+\mu_0)]S_{1122}+2k_2(k_0-\mu_0)\}/b_2, \\ h_2 &= \{2[(3k_0-\mu_0)\mu_0-k_2(k_0+\mu_0)]S_{2211}\}/b_2, \\ d_2 &= \{2[(3k_0-\mu_0)\mu_0-k_2(k_0+\mu_0)](1-S_{2222}-S_{2233})+2k_2(k_0+\mu_0)\}/b_2, \\ e_2 &= -1/\left(2S_{2323}+\frac{\mu_0}{\mu_1-\mu_0}\right), \\ f_2 &= -1/(2S_{1212}-1), \\ b_2 &= 2[(3k_0-\mu_0)\mu_0-k_2(k_0+\mu_0)][(1-S_{1111})(1-S_{2222}-S_{2233})-2S_{1122}S_{2211}] \\ &\quad +2(1-S_{1111})k_2(k_0+\mu_0)-2S_{2211}k_2(k_0-\mu_0); \end{aligned} \tag{A.3}$$

but for type-2 debonding in Fig. 1(b)

$$
\begin{aligned}
c_2 &= \{2[(3k_0-\mu_0)\mu_0-n_2k_0](1-S_{1111})+2n_2k_0\}/b_2,\\
g_2 &= 2[(3k_0-\mu_0)\mu_0-n_2k_0]S_{1122}/b_2,\\
h_2 &= 2[(3k_0-\mu_0)\mu_0-n_2k_0]S_{2211}/b_2,\\
d_2 &= 2[(3k_0-\mu_0)\mu_0-n_2k_0](1-S_{2222}-S_{2233})/b_2,\\
e_2 &= 1/(1-2S_{2323}),\\
f_2 &= 1/(1-2S_{1212}),\\
b_2 &= 2[(3k_0-\mu_0)\mu_0-n_2k_0][(1-S_{1111})(1-S_{2222}-S_{2233})-2S_{1122}S_{2211}]\\
&\quad -2[(1-S_{2222}-S_{2233})k_0-S_{1122}\mu_0]n_2.
\end{aligned}
\tag{A.4}
$$

For spherical inclusions, the above equation can be simplified to

$$
\begin{aligned}
c_1 &= \frac{3(1-\nu_0)}{1-2\nu_0}\{-(1-2\nu_0)(7-5\nu_0)(1+\nu_1)\mu_1^2+[3(1+\nu_0)(1-\nu_1)\\
&\quad +(10\nu_0(1-\nu_0)-4)(1+\nu_1)]\mu_1\mu_0+2(1+\nu_0)(4-5\nu_0)(1-2\nu_1)\mu_0^2\}/b_1,\\
g_1 &= -\frac{3(1-\nu_0)}{1-2\nu_0}\{(1-2\nu_0)(1-5\nu_0)(1+\nu_1)\mu_1^2+[4(4-4\nu_0-\nu_0^2)\nu_1\\
&\quad -2(1+2\nu_0-5\nu_0^2)]\mu_1\mu_0+(1+\nu_0)(1-5\nu_0)(1-2\nu_1)\mu_0^2\}/b_1\\
h_1 &= g_1\\
d_1 &= \frac{9(1-\nu_0)}{1-2\nu_0}\{-2(1-2\nu_0)(1+\nu_1)\mu_1^2-[(1-3\nu_0)-(3-3\nu_0-10\nu_0^2)\nu_1]\mu_1\mu_0\\
&\quad +(1+\nu_0)(3-5\nu_0)(1-2\nu_1)\mu_0^2\}/b_1,\\
e_1 &= -1/\left[\frac{2(4-5\nu_0)}{15(1-\nu_0)}+\frac{\mu_0}{\mu_1-\mu_0}\right],\\
f_1 &= e_1,\\
b_1 &= 2(1+\nu_0)(4-5\nu_0)(1+\nu_1)\mu_1^2+(1+\nu_0)[(23-25\nu_0)-5(5-7\nu_0)\nu_1]\mu_1\mu_0\\
&\quad +2(1-2\nu_1)(7-5\nu_0)(1+\nu_0)\mu_0^2,
\end{aligned}
\tag{A.5}
$$

and, for the type-1 debonding

$$
\begin{aligned}
c_2 &= 5(1-\nu_0)(7-5\nu_0)[4(1+\nu_0)(1-\nu_1^2)\mu_0-(1-\nu_0)\mu_1]/b_2,\\
g_2 &= -5(1-\nu_0)[4(1+\nu_0)(1-5\nu_0)(1-\nu_1^2)\mu_0-(1-\nu_0)(1+10\nu_0)\mu_1]/b_2,\\
h_2 &= -5(1-\nu_0)[4(1+\nu_0)(1-5\nu_0)(1-\nu_1^2)\mu_0-(1-\nu_0)(1-5\nu_0)\mu_1]/b_2,\\
d_2 &= 5(1-\nu_0)[4(1+\nu_0)(4-5\nu_0)(1-\nu_1^2)\mu_0-(1-\nu_0)(7-5\nu_0)\mu_1]/b_2,\\
e_2 &= -1/\left[\frac{2(4-5\nu_0)}{15(1-\nu_0)}+\frac{\mu_0}{\mu_1-\mu_0}\right],\\
f_2 &= 1/\left[1-\frac{2(4-5\nu_0)}{15(1-\nu_0)}\right],\\
b_2 &= 24(1+\nu_0)(4-5\nu_0)(1-\nu_1^2)\mu_0-(1-\nu_0)(17-20\nu_0-25\nu_0^2)\mu_1\,;
\end{aligned}
\tag{A.6}
$$

but for the type-2 debonding

$$
\begin{aligned}
c_2 &= 5(1-\nu_0)[(7-5\nu_0)E_0+2(4-5\nu_0)E_1]/b_2,\\
g_2 &= 5(1-\nu_0)(1-5\nu_0)(E_1-E_0)/b_2,\\
h_2 &= 5(1-\nu_0)[(1+10\nu_0-15\nu_0^2)E_1-(1-5\nu_0)E_0]/b_2,\\
d_2 &= -10(1-\nu_0)[(4-5\nu_0)(E_1-E_0)]/b_2,\\
e_2 &= \frac{15(1-\nu_0)}{7-5\nu_0},\\
f_2 &= \frac{15(1-\nu_0)}{7-5\nu_0},\\
b_2 &= 2\{3(3-5\nu_0)E_0-[5(1-\nu_0^2)(1-5\nu_0)+6]E_1\}.
\end{aligned}
\tag{A.7}
$$